

## Precise edge functionalization and tailoring of graphene via solvent-controlled reactions

Mingyao Li<sup>a,1</sup>, Shuyao Zhou<sup>a,1</sup>, Shizhao Ren<sup>a,c</sup>, Lei Zhang<sup>a</sup>, Bing Yin<sup>a</sup>, Cong Zhao<sup>b</sup>, Zhirong Liu<sup>a</sup>, Chuancheng Jia<sup>a,b,\*\*</sup>, Xuefeng Guo<sup>a,b,\*</sup>

<sup>a</sup> Beijing National Laboratory for Molecular Sciences, National Biomedical Imaging Center, College of Chemistry and Molecular Engineering, Peking University, 292 Chengfu Road, Haidian District, Beijing, 100871, PR China

<sup>b</sup> Center of Single-Molecule Sciences, Institute of Modern Optics, Tianjin Key Laboratory of Microscale Optical Information Science and Technology, Frontiers Science Center for New Organic Matter, College of Electronic Information and Optical Engineering, Nankai University, Tianjin, 300350, PR China

<sup>c</sup> School of Resources and Chemical Engineering, Sanming University, Sanming, Fujian, 365004, PR China

### ARTICLE INFO

#### Keywords:

Graphene  
Friedel-Crafts acylation  
Precise edge functionalization  
Quantum dot  
Solvent effect

### ABSTRACT

Controllable edge-selective modification and tailoring of graphene are particularly critical for graphene applications. In this study, precise edge functionalization and tailoring of graphene are realized by a solvent-controlled Friedel-Crafts acylation reaction. Specifically, experimental and theoretical studies demonstrate that solvent effects can effectively control the reaction pathways of substituent and ionic mechanisms. Under the substituent mechanism, carboxyl groups are accurately introduced to the edge of graphene, which can be used as new reaction sites for further modification. Under the ionic mechanism, the acylation process can further tear graphene to the desired size. When the reaction is sufficient, graphene can be torn into highly dispersed high-quality quantum dots on a scale of 5 nm. This edge- and size-controllable fabrication method expands potential applications of graphene, such as electronic devices, semiconductors, catalysis and batteries.

### 1. Introduction

Graphene, a two-dimensional (2D) material with  $sp^2$ -hybridized aromatic carbon, is a unique material that has been extensively studied. Due to its good performance, graphene is expected to be used in various applications such as electronic devices [1,2], energy storage [3], and catalyst [4]. However, the chemical inertness and random size of graphene restrict its further development. To better realize the applications of graphene in various fields, it needs to be effectively modified and tailored.

Graphene can be viewed as an extension of X and Y axes of benzene, making it possible to modify graphene using traditional organic chemical reactions [5,6]. Various methods have been explored to modify and tailor graphene to enrich its functionality of graphene. Some organic reactions have been confirmed to occur at the edge or basal plane of

graphene, such as Diels-Alder reaction [7], 1,3-dipolar cycloaddition [8], and diazonium reaction [9,10]. For the tailoring of graphene, some severe methods are usually required, such as laser fragmentation [11, 12] and strong oxidation cutting [13,14]. These methods require either high-energy lasers or strong oxidant such as  $H_2O_2$  [15],  $HNO_3$  [14], and oxone [16], whose poor controllability damages graphene. Therefore, there is a need to develop efficient methods to achieve controllable edge functionalization and tailoring of graphene.

Friedel-Crafts acylation reaction is a well-known organic reaction in which hydrogen atoms of aromatic hydrocarbons are replaced by acyl groups in the presence of Lewis acids. In the field of graphene modification, Friedel-Crafts acylation reaction has been used for edge-selective functionalization of graphene via an ionic mechanism [17,18]. However, it is generally accepted that ionic and substituent mechanisms are two possible pathways for Friedel-Crafts acylation reaction [19]. In this

\* Corresponding author. Beijing National Laboratory for Molecular Sciences, National Biomedical Imaging Center, College of Chemistry and Molecular Engineering, Peking University, 292 Chengfu Road, Haidian District, Beijing, 100871, PR China.

\*\* Corresponding author. Center of Single-Molecule Sciences, Institute of Modern Optics, Tianjin Key Laboratory of Microscale Optical Information Science and Technology, Frontiers Science Center for New Organic Matter, College of Electronic Information and Optical Engineering, Nankai University, Tianjin, 300350, PR China.

E-mail addresses: [jiacc@nankai.edu.cn](mailto:jiacc@nankai.edu.cn) (C. Jia), [guoxf@pku.edu.cn](mailto:guoxf@pku.edu.cn) (X. Guo).

<sup>1</sup> These authors contributed equally to this work.

<https://doi.org/10.1016/j.carbon.2022.06.072>

Received 28 April 2022; Received in revised form 21 June 2022; Accepted 27 June 2022

Available online 5 July 2022

0008-6223/© 2022 Elsevier Ltd. All rights reserved.

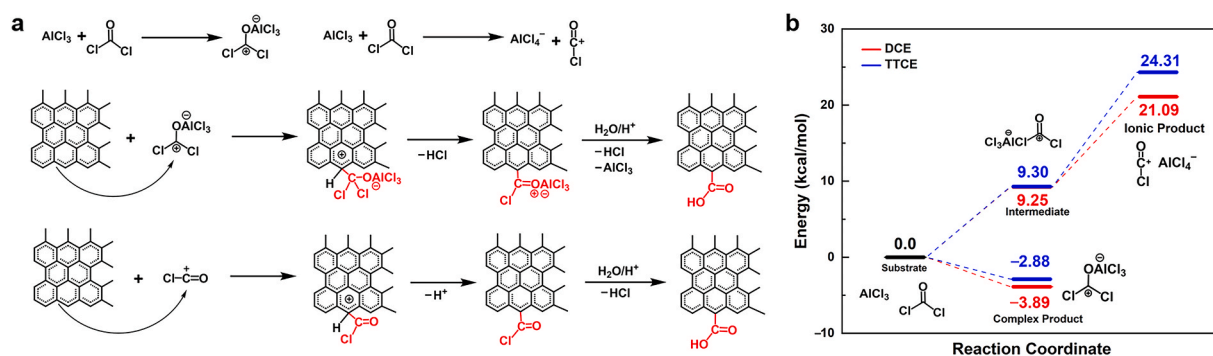


**Fig. 1.** Mechanism of Friedel-Crafts acylation reaction of graphene. (a) Oxonium complex based nucleophilic substitution mechanism and ion pair based ionic mechanism for two Friedel-Crafts acylation reaction pathways. (b) Energy profiles for the formation of oxonium complex or ion-pair in TTCE or DCE, respectively. (A colour version of this figure can be viewed online.)

work, solvent effects are exploited to control these reaction mechanism pathways for precise edge functionalization and tailoring of graphene. In tetrachloroethane (TTCE), the reaction proceeds mainly through the substituent mechanism, enabling precise edge functionalization with carboxyl groups. In dichloroethane (DCE), the reaction proceeds mainly through the ionic mechanism, and graphene is controllably torn apart. With the sufficient tearing reaction, uniformly dispersible graphene quantum dots (GQDs) can be prepared. The active edge and controllable size of the as-prepared graphene will facilitate its applications in sensing, optoelectronic devices, catalysis and energy storage.

## 2. Materials and methods

### 2.1. Materials

Graphene was purchased from Cheap Tubes Inc. Aluminium chloride (99%) was purchased from Alfa Aesar. Oxalyl chloride, 2.0 M solution in dichloromethane, was purchased from Acros. Ultra-dry 1,2-Dichloroethane (DCE, 99.5%) was obtained from J&K. 1,1,2,2-Tetrachloroethane (TTCE, >97%) was ordered from TCI.

### 2.2. Preparation of modified graphene

12.56 mmol aluminium chloride, 6.4 mmol oxalyl chloride and 80 mg graphene were stirred in DCE/TTCE under argon atmosphere in a 250 mL three-necked flask with a reflux condenser. Oxalyl chloride (6.4 mmol, 3.2 mL) was added dropwise under the condition of ice water bath for 1 h.

Then, it was placed in a constant temperature oil bath. In DCE, reactions were carried out at room temperature, 40 °C, 60 °C and 80 °C for 18 h. In TTCE, reactions were carried out at 80 °C, 100 °C and 120 °C, respectively. All the reactions were quenched with glacial hydrochloric acid. The turbid liquid was filtered by using a Buchner funnel. The resultants were washed by ethyl chloride, methanol, and water various times to obtain modified graphene, and dried in a vacuum oven at 170 °C for 5 days. After all, products in DCE for different temperatures were called MG-RT-18-DCE, MG-40-18-DCE, MG-60-18-DCE, and MG-80-18-DCE. Products in TTCE for different temperature were called MG-80-18-TTCE, MG-100-18-TTCE, MG-120-18-TTCE.

When Friedel-Crafts acylation reaction was carried out in DCE for 18 h at 80 °C, the graphene was tailored into small pieces, forming relatively stable GQDs. It is expected that the products consisted of a mixture of ultrasmall GQDs, so the further purification was executed. Specifically, the mixture was centrifuged in THF at 12000 r/min for 20 min. Then, the precipitate is redissolved into THF and centrifuged at 8000 r/min. GQDs with certain sizes in the supernatant were obtained by repeating the centrifugation processes three times.

### 2.3. Characterization

Thermogravimetric analysis (TGA) were recorded on a TA Q600 SDT (TA Instrument) in two steps: firstly, the temperature was raised from room temperature to 1000 °C at a heating rate of 50 °C/min under nitrogen atmosphere; secondly, after cooling to room temperature, the temperature was raised to 1000 °C in air atmosphere at a heating rate of 10 °C/min. A thermogravimetric analyzer coupled with Fourier transform infrared analysis (TG-FTIR) was carried out on hyphenation of TG/FTIR/GCMS from PerKinElmer. X-ray photoelectron spectra (XPS) were conducted on AXIS Supra. The scanning electron microscopy (SEM) was employed in Hitachi S-4800. The high-resolution transmission electron microscopy (HR-TEM) was performed in JEM-2100F microscope operating at 200 kV.

### 2.4. Theoretical calculation

All the computational works were implemented in Gaussian16 software. The SMD implicit solvation model was adopted to simulate the dichloroethane and tetrachloroethane solvent environments. For the energy profiles of formation of acylium chloride cation and the complex molecule, the geometries of species were optimized at B3LYP/6–311 + g (d,p) level, and the single-point energies were calculated at the same level. For the energy profiles of etching process of the polycyclic aromatic hydrocarbon molecule, the chloride anion was optimized at m062x/6–31 + g(d) level, while geometries of other species were optimized at m062x/6–31g(d). The single point energies were calculated at m062x/6–311 + g(d,p) level.

## 3. Results and discussion

### 3.1. Solvent-controlled reaction pathways

In Friedel-Crafts acylation reaction, aluminum chloride is the commonly used catalyst with good catalytic activity and oxalyl chloride is used as reactant. Oxalyl chloride is decomposed into a mixture of phosgene and carbon monoxide under the action of aluminum chloride. Subsequently, phosgene interacts with aluminum chloride mainly to form oxonium complex and ion pair, which further participate in the reactions according to ionic and nucleophilic substitution mechanisms (Fig. 1a). For the ionic mechanism, the edges of graphene are attacked by highly reactive acyl cations ( $\text{COCl}^+$ ) generated from acid chlorides. For the substituent mechanism, the edges of graphene are attacked by the less reactive complexes ( $\text{COCl}_2\text{-AlCl}_3$ ) formed by acyl chlorides and aluminum chloride [19]. The effects of TTCE and DCE solvents on Friedel-Crafts acylation reaction are further investigated by theoretical simulations. The energy profiles (Fig. 1b) show that the formation of complex with strong electrophiles is thermodynamically preferred due

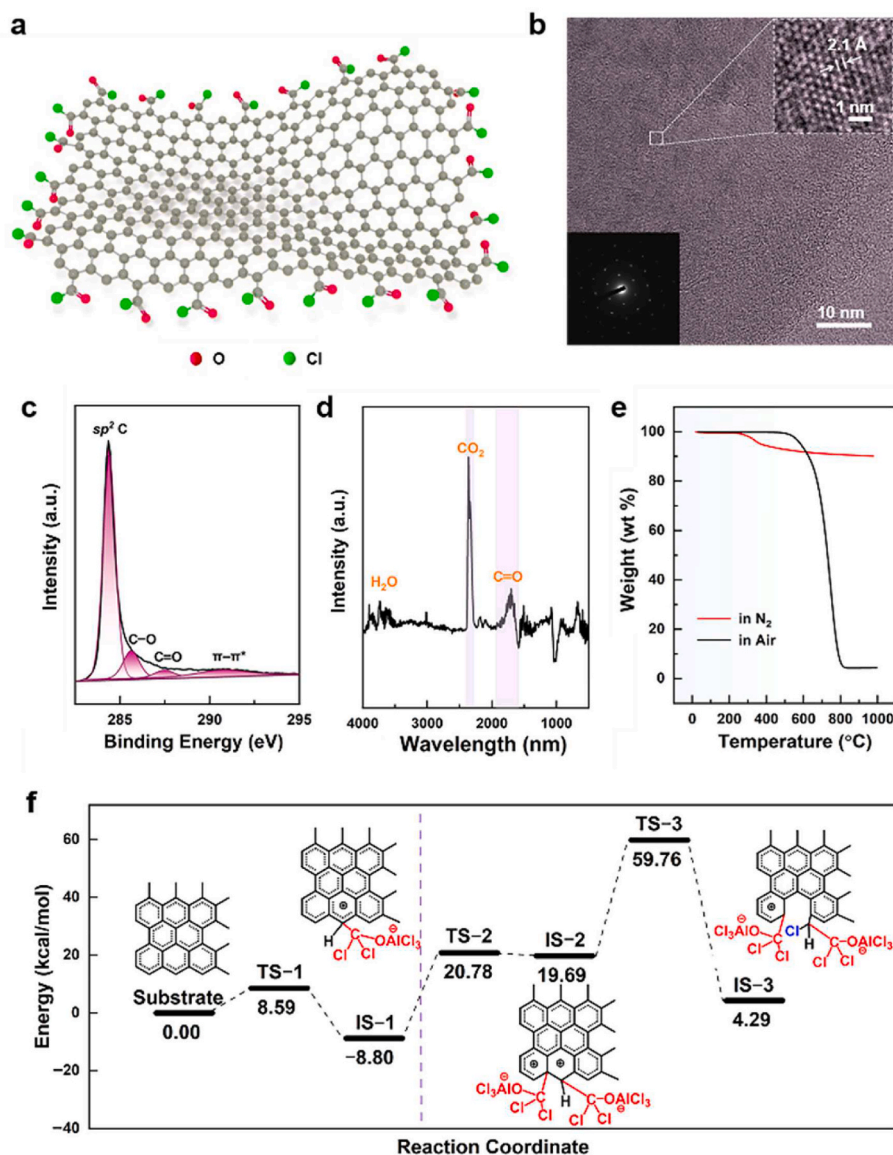


**Fig. 2.** Friedel-Crafts acylation reaction in TTCE. (a) Schematic illustration of edge-selective functionalization of graphene. (b) High-resolution TEM image of modified graphene. Insets show a magnified view of a representative position of graphene (top right) and the corresponding SEAD pattern (bottom left) of modified graphene. (c) XPS spectrum of modified graphene. (d) IR spectrum of species released from modified graphene at 702 °C. (e) TGA of modified graphene under nitrogen atmosphere (red line) and air atmosphere (black line). (f) Energy profiles for the reaction with  $COCl_2 \cdot AlCl_3$  complex. (A colour version of this figure can be viewed online.)

to the reduced Gibbs free energy. The energy barriers of this reaction pathway are not very different in different solvents. However, for another pathway with forming a highly reactive acyl cation, the energy barrier in TTCE is 3.22 kcal/mol higher than that in DCE. Based on transition state theory, the reaction rate constant ( $k$ ) can be calculated from these reaction energy barriers from the following equation:

$$k = \kappa \frac{k_B T}{h} e^{-\frac{\Delta G^\ddagger}{RT}}$$

The energy barrier difference leads to that the rate of  $COCl^+$  generation should be  $\sim 99$  times faster in DCE than in TTCE. Furthermore,  $COCl^+$  can be more stable in DCE due to its larger polarity and smaller size.  $COCl^+$  is expected to be the main reactant in DCE. Therefore, the solvent can effectively regulate the production of highly reactive cations, providing a basis for further regulating of the reaction by the solvent.

### 3.2. Edge-selective carboxylation of graphene

In TTCE, the Friedel-Crafts acylation reaction of graphene was carried out at 80 °C for 18 h under the catalysis of aluminum trichloride. After that, the reaction was quenched with glacial hydrochloric acid to

form the carboxyl groups. By X-ray photoelectron spectroscopy (XPS) characterization (Figs. 2c and S1), it can be observed that the oxygen atom content of functionalized graphene increased from 2.59% to 24% in comparison with pristine graphene, indicating the presence of carboxyl groups. Specifically, the high resolution C1s peak can be deconvoluted into three bands at  $\sim 284.6$  eV,  $\sim 287.0$  eV and  $\sim 288.9$  eV, which are assigned to  $sp^2$  C=C, C-O and C=O bonds, respectively [20–22]. Carboxylated graphene was further confirmed by thermogravimetry-Fourier transform infrared spectroscopy (TG-FTIR). During the heating program, the functional group information is displayed (Fig. 2d). The band at  $1684\text{ cm}^{-1}$  is assigned to the C=O stretching vibrations of carboxylated graphene [23]. Double peaks at  $2182\text{ cm}^{-1}$  and  $2094\text{ cm}^{-1}$  are attributed to CO gas [24]. In addition, the concentration of  $CO_2$  gradually increases with increasing temperature, indicating that a decarboxylation process takes place. To confirm the amount of functionalization, thermogravimetric analysis (TGA) of the functionalized graphene was performed under nitrogen atmosphere. As shown in Fig. 2e (red line), the  $\sim 10\%$  weight loss of the first step at  $\sim 220$  °C is attributed to covalent functionalization [25]. The quantity of functional groups increases as the reaction temperature increases (Fig. S2).

To determine the effect of the reaction on the graphene framework

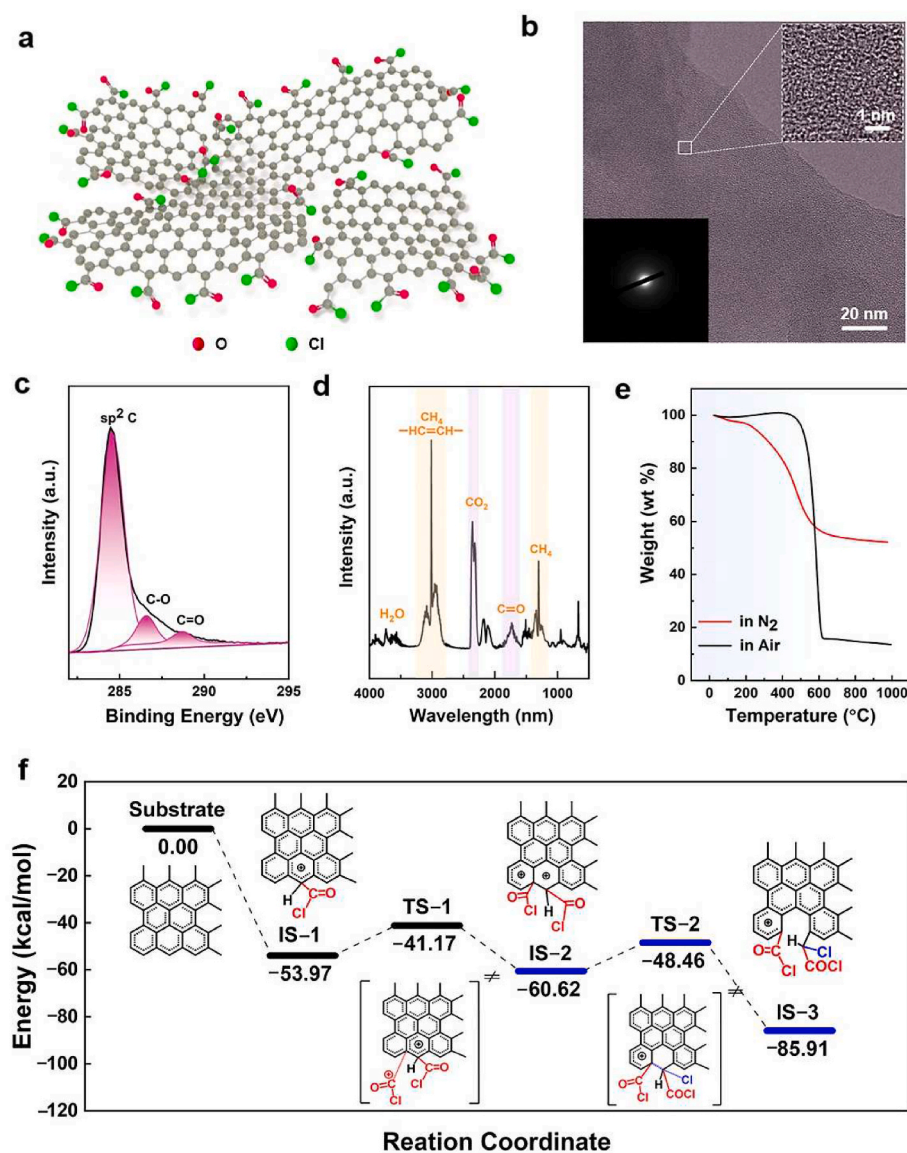


**Fig. 3.** Friedel-Crafts acylation reaction in DCE. (a) Schematic illustration of graphene tearing. (b) High-resolution TEM image of modified graphene. Insets show a magnified view (top right) and SAED pattern (bottom left) of modified graphene. (c) XPS spectrum of the graphene. (d) IR spectrum of species released from modified graphene at 554 °C. (e) TGA of modified graphene under nitrogen atmosphere (red line) and air atmosphere (black line). (f) Energy profiles for the reaction with  $\text{COCl}^+$  cation, highlighting the process of graphene tailoring. (A colour version of this figure can be viewed online.)

structure, high-resolution transmission electron microscopy (HRTEM) characterization was used. A clear lattice structure of the functionalized graphene can be observed (Fig. 2b), which shows the structural characteristics of honeycomb hexagonal unit cells. Selected area electron diffraction (SAED) patterns also show that the graphene both before and after modification in TTCE have high crystallinity (Fig. S7) [26]. On a large scale, scanning electron microscopy (SEM) characterization shows that the morphology of functionalized graphene is well preserved after modification in TTCE (Fig. S5). Furthermore, the XPS peak of the sample at  $\sim 291.4$  eV (Fig. 2c) is assigned to the  $\pi$ - $\pi^*$  vibrational satellite, which proves that the basal plane structure is intact [27,28]. In an air atmosphere, the complete combustion temperature of the sample is  $\sim 800$  °C (Fig. 2e), which is the same as that of graphene lattice carbon [29]. All above characterizations confirm that the modified graphene in TTCE maintains the intact framework structure, so that the functional groups are successfully modified at the edge of graphene without any damage to the basal plane (Fig. 2a).

To understand the experimental phenomenon of edge-selective functionalization, the  $\text{COCl}_2\text{-AlCl}_3$  complex is expected to be the main reactant in TTCE, which is further explored by theoretical calculations. Here, polycyclic aromatic hydrocarbon (PAH), as a fragment of graphene, is used to simulate to react with the complex (Fig. 2f). Firstly, the

carbon atom at the edge is attacked by the  $\text{COCl}_2\text{-AlCl}_3$  complex, which crosses a low potential barrier of  $\sim 8.59$  kcal/mol. For further reaction, the potential barrier for complex to attack the neighboring carbon is as high as  $\sim 29.58$  kcal/mol, which is difficult to cross. When this complex attack further leads to C-C bond cleavage, an additional barrier of  $\sim 40.07$  kcal/mol needs to be crossed, preventing the corresponding step from taking place. Therefore, according to the above analysis, the precise edge-selective modification occurs through a substituent mechanism, which can be controlled by the solvent effect of TTCE.

### 3.3. Novel phenomena in Friedel-Crafts acylation reaction of graphene

When DCE is used as the solvent, the reaction was also carried out at 80 °C for 18 h, which is the same experimental conditions as TTCE. The Cl1s peaks of C-O and C=O bonds in XPS (Fig. 3c) and the C=O stretching vibration of TGA-IR at  $\sim 1684$   $\text{cm}^{-1}$  (Fig. 3d) indicate carboxyl functionalization [30,31], which is consistent with the results in DCE. TGA trace shows a  $\sim 50\%$  mass loss under nitrogen atmosphere (Fig. 3e) due to desorption of the modified functional groups, indicating a further reaction in DCE. Through HRTEM characterization, it is confirmed that amorphous carbon without diffraction spots is formed (Figs. 3b and S8) [32,33]. Under the air atmosphere, the carbon element of graphene is

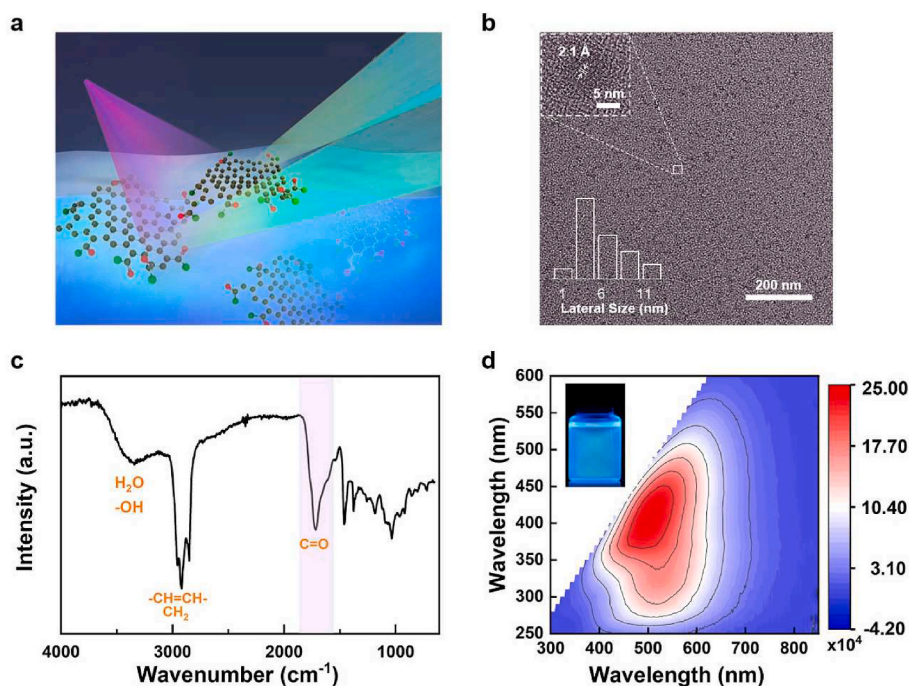


**Fig. 4.** GQDs chemically tailored from graphene. (a) Schematic illustration of GQDs with photoluminescence. (b) High-resolution TEM image of GQDs. Inset shows a magnified view of a GQD and the corresponding size distribution. (c) FTIR spectrum of GQDs. (d) PL mapping of GQD dispersions in THF. Inset shows the photograph of the GQD solution excited at 365 nm. (A colour version of this figure can be viewed online.)

completely burned out at a relatively lower temperature of 600 °C, which indicates the existence of highly reactive carbon (Fig. 3e). Furthermore, the disappearance of the satellite peaks in the XPS spectrum (Fig. 3c and Fig. S1) indicates that the large  $\pi$  system of graphene is disrupted. In the TG-FTIR spectrum (Fig. 3d and Fig. S4), new peaks of olefin at 3078  $\text{cm}^{-1}$  and  $\text{CH}_2$  at 1300  $\text{cm}^{-1}$  appear [34,35], which further prove that some basal plane of graphene is broken into fragments. Therefore, a vigorous modification reaction with graphene tearing occurs in DCE.

To further explore the mechanism of Friedel-Crafts acylation reaction in DCE, the temperature-dependent reaction from room temperature to 80 °C were investigated. According to SEM characterizations (Fig. S6), it can be observed that the morphology of graphene remains flat after reaction at room temperature. As the reaction temperature increases, the wrinkles gradually extend from the edge to the basal plane, which is due to the deformation caused by the deepening of the reaction. Furthermore, less weight loss on heating under nitrogen in TGA indicates weaker modification of the samples prepared at room temperature (Fig. S2). The carbon element of the modified graphene is completely burned out at ~800 °C, which is the same as the burning temperature of graphene. HRTEM characterization further confirms that the reaction only occurs at the edge of graphene without any damage to the basal plane. As the reaction temperature increases, the degree of modification gradually increases (Fig. S7), which can be confirmed by TGA (Fig. S2). In addition, at the lower reaction temperature of 40 °C and 60 °C, there are two forms of carbon in the modified graphene (Fig. S2). One is lattice graphene that burns at ~800 °C, and the other is amorphous carbon graphene that burns at ~600 °C. Further HRTEM characterization shows that the amorphous carbon produced by the reaction increases from the edge as the reaction temperature increases (Fig. 3b and Fig. S8). These suggest that a barrier needs to be crossed for the tearing reaction to occur, and that the reaction can be regulated by temperature.

For the reaction mechanism in DCE, as confirmed by the above theoretical simulations,  $\text{COCl}^+$  is stable and abundant in DCE and is expected to be the main reactant. During the reaction (Fig. 3f), the first

$\text{COCl}^+$  attacks the edge carbon of graphene without any potential barrier. Then, the second  $\text{COCl}^+$  reacts with the adjacent carbon, crossing an energy barrier of ~12.80 kcal/mol. After that,  $\text{Cl}^-$  attacks the positive carbon to break the C–C bond by crossing a barrier of ~12.16 kcal/mol. The energy barrier for each step is low enough that the C–C bonds at the edges can be broken, causing the graphene to tear. The structural evolution can be evaluated by Raman spectra. In particular, the intensity ratio of D-band to G-band ( $I_D/I_G$ ) can illustrate the modification degree of graphene. As the reaction temperature increases, the  $I_D/I_G$  ratio increases from ~0.24 to ~0.89, which indicates the growing degree of graphene modification. When the reaction temperature reaches up to 80 °C, there is no band in Raman spectra, showing that the graphene is totally cleaved into GQDs (Fig. S9). Correspondingly, Friedel-Crafts acylation reaction with  $\text{COCl}^+$  cations in DCE solvent can tailor graphene into fragments with disrupting the lattice structure of graphene (Fig. 3a).

### 3.4. Formation of GQDs

After a thorough reaction in DCE, the  $\text{COCl}^+$  was further introduced to the system to break graphene into fragments and lead to the formation of GQDs. HRTEM images (Fig. 4b) show that the prepared GQDs have the mono-dispersity and an intact graphene lattice structure. The size distribution of GQDs is 1–13 nm with an average lateral size of ~5 nm. Through further FTIR characterization, the characteristic stretching vibration bands for  $-\text{OH}$  at ~3343  $\text{cm}^{-1}$ ,  $-\text{C}=\text{O}$  at ~1717  $\text{cm}^{-1}$  and  $sp^2$   $\text{C}=\text{C}$  at ~1460  $\text{cm}^{-1}$  prove that GQDs with conjugated components are functionalized with  $-\text{COOH}$  groups (Fig. 4c) [13,36]. The functional  $-\text{COOH}$  group enables the GQDs to have good dispersibility in tetrahydrofuran (THF), and the GQDs can exhibit uniform bright blue photoluminescence (PL) under 365 nm excitation light. Furthermore, the GQDs suspension exhibits ultra-high stability and maintains strong PL properties even after 2 years in the air. The reason for the long-term structural stability of GQDs is that GQDs are functionalized with  $\text{COOH}$ , which prevents oxidation and coagulation. On one hand, the  $\text{COOH}$  groups reduce the fragile dangling bonds at the edge of GQDs,

thereby avoiding further oxidation by oxygen. GQDs obtained by tailoring from the edge region of graphene have the stable and intact graphene lattice structure. On the other hand, owing to the solvation effect, GQDs with COOH groups have good solubility in polar solvents. In addition, due to the electric repulsion of ionized COOH groups, GQDs keep away from each other to avoid further polymerization, which largely improves the thermodynamic stability. The PL emission spectra of these GQDs exhibit excitation-dependent behavior (Fig. 4a and d) [37]. When the excitation wavelength is changed from 250 nm to 600 nm, the PL peak position is red-shifted from ~488 nm to ~630 nm (Fig. 4d), enabling tunable emission by adjusting the excitation wavelength. Under excitation at 410 nm, the strongest PL appears at ~509 nm with an efficiency of ~2.39%.

#### 4. Conclusion

In summary, this study has realized precise controllable edge modification and size-controlled tailoring of graphene via Friedel-Crafts acylation. Based on the solvent effect, Friedel-Crafts acylation reaction can be controllably carried out in different solvents under ionic or substituent mechanism. Under the substitution mechanism in TTCE, edge carboxylated graphene is generated while maintaining the intrinsic skeleton structure of graphene. Under the ionic mechanism in DCE, graphene can be well tailored through temperature control by breaking C–C bonds from the edges. Therefore, size-controllable modified graphene to form uniform GQDs with bright PL can be prepared, providing a basis for further applications such as bioluminescent labeling in the field of multicolor imaging biology.

#### CRediT authorship contribution statement

**Mingyao Li:** Conceptualization, Methodology, Writing – original draft. **Shuyao Zhou:** Software, Data curation, Writing – original draft. **Shizhao Ren:** Conceptualization, Data curation, Formal analysis. **Lei Zhang:** Methodology, Data curation, Formal analysis. **Bing Yin:** Structure of the materials, Formal analysis. **Cong Zhao:** Methodology, Data curation. **Zhirong Liu:** Software, Data curation. **Chuancheng Jia:** Supervision, Conceptualization, Writing – review & editing. **Xuefeng Guo:** Supervision, Conceptualization, Writing – review & editing.

#### Declaration of competing interest

The authors declare that they have no known competing financial interests or personal relationships that could have appeared to influence the work reported in this paper.

#### Acknowledgements

The authors acknowledge primary financial supports from the National Key R&D Program of China (2017YFA0204901, 2021YFA1200101 and 2021YFA1200102), the National Natural Science Foundation of China (22150013, 22173050, 21727806 and 21933001), the Tencent Foundation through the XPLOER PRIZE, “Frontiers Science Center for New Organic Matter” at Nankai University (63181206), the Natural Science Foundation of Beijing (2222009) and Beijing National Laboratory for Molecular Sciences (BNLMS202105).

#### Appendix A. Supplementary data

Supplementary data to this article can be found online at <https://doi.org/10.1016/j.carbon.2022.06.072>.

#### References

- [1] N.O. Weiss, H. Zhou, L. Liao, Y. Liu, S. Jiang, Y. Huang, X. Duan, Graphene: an emerging electronic material, *Adv. Mater.* 24 (2012) 5782–5825.

- [2] Z. Chen, A. Narita, K. Müllen, Graphene Nanoribbons: on-surface synthesis and integration into electronic devices, *Adv. Mater.* 32 (2020), 2001893.
- [3] J. Zhu, D. Yang, Z. Yin, Q. Yan, H. Zhang, Graphene and graphene-based materials for energy storage applications, *Small* 10 (2014) 3480–3498.
- [4] C. Shan, H. Tang, T. Wong, L. He, S.-T. Lee, Facile synthesis of a large quantity of graphene by chemical vapor deposition: an advanced catalyst carrier, *Adv. Mater.* 24 (2012) 2491–2495.
- [5] C.N.R. Rao, A.K. Sood, K.S. Subrahmanyam, A. Govindaraj, Graphene: the new two-dimensional nanomaterial, *Angew. Chem. Int. Ed.* 48 (2009) 7752–7777.
- [6] T. Wassmann, A.P. Seitsonen, A.M. Saitta, M. Lazzeri, F. Mauri, Clar’s theory,  $\pi$ -electron distribution, and geometry of graphene nanoribbons, *J. Am. Chem. Soc.* 132 (2010) 3440–3451.
- [7] S. Sarkar, E. Bekyarova, S. Niyogi, R.C. Haddon, Diels-Alder chemistry of graphite and graphene: graphene as diene and dienophile, *J. Am. Chem. Soc.* 133 (2011) 3324–3327.
- [8] M. Quintana, K. Spyrou, M. Grzelczak, W.R. Browne, P. Rudolf, M. Prato, Functionalization of graphene via 1,3-dipolar cycloaddition, *ACS Nano* 4 (2010) 3527–3533.
- [9] J.R. Lomeda, C.D. Doyle, D.V. Kosynkin, W.-F. Hwang, J.M. Tour, Diazonium functionalization of surfactant-wrapped chemically converted graphene sheets, *J. Am. Chem. Soc.* 130 (2008) 16201–16206.
- [10] E. Bekyarova, M.E. Itkis, P. Ramesh, C. Berger, M. Sprinkle, W.A. de Heer, R. C. Haddon, Chemical modification of epitaxial graphene: spontaneous grafting of aryl groups, *J. Am. Chem. Soc.* 131 (2009) 1336–1337.
- [11] S. Kang, K.H. Jung, S. Mhin, Y. Son, K. Lee, W.R. Kim, H. Choi, J.H. Ryu, H. Han, K. M. Kim, Fundamental understanding of the formation mechanism for graphene quantum dots fabricated by pulsed laser fragmentation in liquid: experimental and theoretical insight, *Small* 16 (2020), 2003538.
- [12] L. Shen, S. Zhou, F. Huang, H. Zhou, H. Zhang, S. Wang, S. Zhou, Nitrogen-doped graphene quantum dots synthesized by femtosecond laser ablation in liquid from laser induced graphene, *Nanotechnology* 33 (2021), 115602.
- [13] D. Pan, J. Zhang, Z. Li, M. Wu, Hydrothermal route for cutting graphene sheets into blue-luminescent graphene quantum dots, *Adv. Mater.* 22 (2010) 734–738.
- [14] Z. Luo, G. Qi, K. Chen, M. Zou, L. Yuwen, X. Zhang, W. Huang, L. Wang, Microwave-assisted preparation of white fluorescent graphene quantum dots as a novel phosphor for enhanced white-light-emitting diodes, *Adv. Funct. Mater.* 26 (2016) 2739–2744.
- [15] R. Tian, S. Zhong, J. Wu, W. Jiang, Y. Shen, W. Jiang, T. Wang, Solvothermal method to prepare graphene quantum dots by hydrogen peroxide, *Opt. Mater.* 60 (2016) 204–208.
- [16] Y. Shin, J. Park, D. Hyun, J. Yang, J.-H. Lee, J.-H. Kim, H. Lee, Acid-free and oxone oxidant-assisted solvothermal synthesis of graphene quantum dots using various natural carbon materials as resources, *Nanoscale* 7 (2015) 5633–5637.
- [17] J.-M. Seo, L.-S. Tan, J.-B. Baek, Defect/edge-selective functionalization of carbon materials by “direct” Friedel-Crafts acylation reaction, *Adv. Mater.* 29 (2017), 1606317.
- [18] E.-K. Choi, I.-Y. Jeon, S.-Y. Bae, H.-J. Lee, H.S. Shin, L. Dai, J.-B. Baek, High-yield exfoliation of three-dimensional graphite into two-dimensional graphene-like sheets, *Chem. Commun.* 46 (2010) 6320–6322.
- [19] P.H. Gore, The Friedel-Crafts acylation reaction and its application to polycyclic aromatic hydrocarbons, *Chem. Rev.* 55 (1955) 229–281.
- [20] A. Ganguly, S. Sharma, P. Papakonstantinou, J. Hamilton, Probing the thermal deoxygenation of graphene oxide using high-resolution in situ X-ray-based spectroscopies, *J. Phys. Chem. C* 115 (2011) 17009–17019.
- [21] M. Tortello, S. Colonna, M. Bernal, J. Gomez, M. Pavese, C. Novara, F. Giorgis, M. Maggio, G. Guerra, G. Saracco, R.S. Gonnelli, A. Fina, Effect of thermal annealing on the heat transfer properties of reduced graphite oxide flakes: a nanoscale characterization via scanning thermal microscopy, *Carbon* 109 (2016) 390–401.
- [22] M.M. Bernal, A. Di Pierro, C. Novara, F. Giorgis, B. Mortazavi, G. Saracco, A. Fina, Edge-grafted molecular junctions between graphene nanoplatelets: applied chemistry to enhance heat transfer in nanomaterials, *Adv. Funct. Mater.* 28 (2018), 1706954.
- [23] J. Osicka, M. Mrlik, M. Ilcikova, B. Hanulikova, P. Urbanek, M. Sedlacik, J. Mosnacek, Reversible actuation ability upon light stimulation of the smart systems with controllably grafted graphene oxide with poly (glycidyl methacrylate) and PDMS elastomer: effect of compatibility and graphene oxide reduction on the photo-actuation performance, *Polymers* 10 (2018) 832.
- [24] M.A.O. Lourenço, M. Fontana, P. Jagdale, C.F. Pirri, S. Bocchini, Improved CO<sub>2</sub> adsorption properties through amine functionalization of multi-walled carbon nanotubes, *Chem. Eng. J.* 414 (2021), 128763.
- [25] S. Guo, Y. Nishina, A. Bianco, C. Menard-Moyon, A flexible method for covalent double functionalization of graphene oxide, *Angew. Chem. Int. Ed.* 59 (2020) 1542–1547.
- [26] A.C. Ferrari, J.C. Meyer, V. Scardaci, C. Casiraghi, M. Lazzeri, F. Mauri, S. Piscanec, D. Jiang, K.S. Novoselov, S. Roth, A.K. Geim, Raman spectrum of graphene and graphene layers, *Phys. Rev. Lett.* 97 (2006), 187401.
- [27] W. Xie, L.-T. Weng, K.M. Ng, C.K. Chan, C.-M. Chan, Clean graphene surface through high temperature annealing, *Carbon* 94 (2015) 740–748.
- [28] Y.-C. Chiang, C.-C. Liang, C.-P. Chung, Characterization of platinum nanoparticles deposited on functionalized graphene sheets, *Materials* 8 (2015) 6484–6497.
- [29] F. Farivar, P.L. Yap, K. Hassan, T.T. Tung, D.N.H. Tran, A.J. Pollard, D. Losic, Unlocking thermogravimetric analysis (TGA) in the fight against “fake graphene” materials, *Carbon* 179 (2021) 505–513.

- [30] J.M. Cervantes-Uc, J.V. Cauich-Rodríguez, H. Vázquez-Torres, A. Licea-Claveríe, TGA/FTIR study on thermal degradation of polymethacrylates containing carboxylic groups, *Polym. Degrad. Stabil.* 91 (2006) 3312–3321.
- [31] H. Yuan, W. Xing, P. Zhang, L. Song, Y. Hu, Functionalization of cotton with UV-cured flame retardant coatings, *Ind. Eng. Chem. Res.* 51 (2012) 5394–5401.
- [32] J. Kotakoski, A.V. Krasheninnikov, U. Kaiser, J.C. Meyer, From point defects in graphene to two-dimensional amorphous carbon, *Phys. Rev. Lett.* 106 (2011), 105505.
- [33] D. Wan, K. Komvopoulos, Transmission electron microscopy and electron energy loss spectroscopy analysis of ultrathin amorphous carbon films, *J. Mater. Res.* 19 (2004) 2131–2136.
- [34] P. Ghosh, M. Das, T. Das, Polyacrylates and acrylate- $\alpha$ -olefin copolymers: synthesis, characterization, viscosity studies, and performance evaluation in lube oil, *Petrol. Sci. Technol.* 32 (2014) 804–812.
- [35] L. Passauer, A case study on the thermal degradation of an acrylate-type polyurethane wood coating using thermogravimetry coupled with evolved gas analysis, *Prog. Org. Coating* 157 (2021), 106331.
- [36] V. Gupta, N. Chaudhary, R. Srivastava, G.D. Sharma, R. Bhardwaj, S. Chand, Luminescent graphene quantum dots for organic photovoltaic devices, *J. Am. Chem. Soc.* 133 (2011) 9960–9963.
- [37] R. Liu, D. Wu, X. Feng, K. Müllen, Bottom-up fabrication of photoluminescent graphene quantum dots with uniform morphology, *J. Am. Chem. Soc.* 133 (2011) 15221–15223.